Available online at www.sciencedirect.com

jmr&t Journal of Materials Research and Technology

journal homepage: www.elsevier.com/locate/jmrt

Original Article

Investigation of the mechanical properties of different amorphous composites using the molecular dynamics simulation

Jiangbo Tang [a,b,**], *A. Ahmadi* [c], *As'ad Alizadeh* [d], *Reza Abedinzadeh* [c,***], *Azher M. Abed* [e], *Ghassan Fadhil Smaisim* [f,g], *Salema K. Hadrawi* [h,i], *Navid Nasajpour-Esfahani* [c], *Davood Toghraie* [c,*]

[a] *School of Engineering, Guangzhou College of Technology and Business, Foshan, Guangdong, 528100, China*
[b] *Institute of New Generation Electronic Information Technology, Guangzhou College of Technology and Business, Foshan, Guangdong, 528100, China*
[c] *Department of Mechanical Engineering, Khomeinishahr Branch, Islamic Azad University, Khomeinishahr, Iran*
[d] *Department of Civil Engineering, College of Engineering, Cihan University-Erbil, Erbil, Iraq*
[e] *Air Conditioning and Refrigeration Techniques Engineering Department, Al-Mustaqbal University College, Babylon, Iraq*
[f] *Department of Mechanical Engineering, Faculty of Engineering, University of Kufa, Iraq*
[g] *Nanotechnology and Advanced Materials Research Unit (NAMRU), Faculty of Engineering, University of Kufa, Iraq*
[h] *Refrigeration and Air-conditioning Technical Engineering Department, College of Technical Engineering, The Islamic University, Najaf, Iraq*
[i] *Computer Engineering Department, Imam Reza University, Mashhad, Iran*

ARTICLE INFO

Article history:
Received 29 August 2022
Accepted 24 February 2023
Available online 2 March 2023

Keywords:
Hardness
Nanocomposite
Al_2O_3 nanoparticle
Molecular dynamics simulation

ABSTRACT

Metal matrix composites have various structural and thermal applications in terms of their unique mechanical and thermal properties compared to their counterparts. These nanoparticle (NP)-reinforced composites have received much attention due to their relatively low production costs and excellent mechanical properties. In the present research, modeling and studying the effects of adding reinforcing NP on the hardness of aluminium-based composites is done using the molecular dynamics (MD) simulation. The expressed structures' equilibration, temperature, and potential energy are calculated and reported in the first simulation stage. In this regard, the parameters of Lennard-Jones potential function for the particles in the MD simulation of aluminium and oxygen. Finally, the results show that the hardness of pure nanocomposite (NC) was equal to 100, and by adding NP with a mass ratio of 6%, the hardness of NC increased from 100 to 190 HV. The radial distribution function (RDF) showed that the composition was in the solid phase at a temperature of 300 K, indicating the proper balance of simulated atomic systems. The

* Corresponding author.
** Corresponding author. School of Engineering, Guangzhou College of Technology and Business, Foshan, Guangdong, 528100, China.
*** Corresponding author.
E-mail addresses: Toghraee@iaukhsh.ac.ir (J. Tang), Abedinzadeh@iaukhsh.ac.ir (R. Abedinzadeh), ggstjb@126.com (D. Toghraie).
https://doi.org/10.1016/j.jmrt.2023.02.193

results show that the maximum value of RDF decreased by increasing the amount of reinforcement. The results show that the yield stress decreased as the volume fraction of reinforcement increased in the crystal structure. Finally, it is expected that the results obtained from MD simulations will be considered in the practical use of aluminium NCs reinforced with alumina nanoparticles in various industrial, engineering and medical uses.

Abbreviations

NP	Nanoparticle
MD	Molecular dynamics
NC	Nanocomposite
RDF	Radial distribution function
Gr	Graphene
GNP	Graphene nanoplatelets
Al	Aluminum
LJ	Lennard-Jones
EAM	Embedded atom model
eV	Electron Volt

Nomenclature

r_i	Position of atom
N	Number of atoms
f	Force
U	Potential energy
F_α	Potential bounded by atom i
ρ_β	Total electron density
ϕ_β	Paired atomic energy

Greek symbols

σ	Potential well's depth
ε	The finite distance at which the potential becomes zero

1. Introduction

The term composite can mean almost anything if taken at face value since all materials are composed of dissimilar subunits if sufficiently examined. However, modern materials engineering usually refers to a "matrix" material reinforced with fibres. Composites are an interesting group of materials that have always attracted the attention of researchers due to their improved or changed properties [1–5]. Amorphous metals are common reinforcements for composites. These metals were a suitable alternative to traditional reinforcements in terms of the special properties they create. Amorphous metals are semi-stable materials with irregular structures and unique mechanical properties [6,7]. Due to the similar structural properties of metals, the presence of metal elements in their structure, and the metal background of composite, the interfaces formed between the reinforcing particles and the background are of high quality, which will significantly improve the mechanical properties of composite [8]. Considering that these metals have advantages such as high corrosion resistance, dimensional stability during use, suitable electrical and thermal conductivity, and application defects such as high density, and low flexibility, one of the methods of improving the mechanical and physical properties of these metals, it is composited with materials that cover its weak points and highlight its strong points [9,10]. Aluminum is a suitable material for composite with metals because it has low density, high flexibility, good corrosion resistance, and high electrical and thermal conductivity [11–16], and for this reason, it is used in various processes such as welding, heat treatment, shaping, and in general in various manufacturing processes. Metal composites are one of the most widely used composites in various industries, such as automotive and aerospace. In some countries, polymer composites are used, which have lower quality, to save money. In advanced countries, the automotive industry use NC and metal composites, which have a much higher quality and are highly resistant to impact and chemical damage, and their weight is also less. Another use of metal-based composites is in the aerospace industry and the construction of racing cars [17].

Many types of research were presented using experimental and MD methods to study the mechanical and thermal behavior of different NCs. For instance, Sun and Simon [18] studied the melting behavior of aluminum NP. They found that as the particle size decreased, the melting response moved to lower temperatures, and the heat of fusion decreased. Prabakaran et al. [19] investigated the freezing behavior of phase change NCs as host matrix based on graphene (Gr) and the effect of volume fraction of graphene nanoplatelets (GNP)/on thermal transfer and rheological behavior of NCs. By increasing the volume fraction to 5%, the thermal conductivities of liquid and solid phases increased by 102% and 46%. Besides, viscosity increased by increasing volume fraction. Parameshwaran et al. [20] studied the thermal and rheological characteristics of hybrid NC phase change materials for thermal energy storage. Rong et al. [21] investigated the strengthening mechanism of GNP/Al composites using MD. The results show that adding a small amount of GNPs led to a significant enhancement in the stiffness and strength of GNP/Al composites. It further revealed that the elasticity and strength enhancement is proportional to GNP Size. Zhang et al. [22] investigated the effects of GNP size on the strengthening mechanism in Al/GNP composites during nano-indentation. They showed that the composite containing the GNP with the maximum size covering the entire matrix showed the highest strength, approximately 1.5 times the value of other all-Gr composites. Lee et al. [23] conducted MD studies on the mechanical properties and deformation mechanism of Gr/Al composites. The mechanical properties of the Gr/Al composite under uniaxial tension and compression were studied using the MD simulation. Yadav et al. [24] studied with the properties of Al matrix composites reinforced with glass NP

with the MD simulation and showed that sample hardness and Young's modulus increased with the increase in volume fraction of MG.

He et al. [25] examined the sintering and mechanical behaviors of Al matrix composites reinforced with GNPs using the MD. The results reveal that adding GNPs improved the thermal performance of composites, as well as the sintering density of nanoparticles, and it depended on the annealing temperature. Mohammadi et al. [26] studied the effect of nanofillers' geometrical aspects on the tribological performance of Al-based NCs. Adnan et al. [27] investigated the effect of filler size on the elastic properties of polymer composites reinforced by NP using the MD simulation. The results show that the elastic properties of NCs dramatically increase by reducing the size of NP. Khorshid et al. [28] investigated the mechanical properties of NCs consisting of a metal matrix and GNP. The results show the proper performance of the powder metallurgy method in producing this category of NCs so that the structures produced had good integrity. Yehia et al. [29] showed that the powder metallurgy method was suitable for preparing mentioned NCs. The results of this research indicate the optimal increase in the hardness value of the studied samples by adding 0.4% of Gr nanoparticles to the primary matrix, which can be considered in industrial applications of NC produced. Moustafa et al. [30] produced GNP based on copper using the powder metallurgy method. The results reveal that by adding 0.8% of NP into the initial copper matrix, the final strength of produced sample reached its maximum value. Arif et al. [31] investigated the morphology and wear of new hybrid NCs based on silica and aluminium made via powder metallurgy. The results showed that the composites reinforced with a 5% SiC volume fraction have the highest wear resistance. Pal et al. [32] investigated the structural and mechanical behavior of Al_2ZrO/metal matrix NCs prepared by the powder metallurgy method. The obtained results showed that by increasing NP, the mechanical properties of metal matrix NCs reinforced with zinc oxide significantly improved. Furthermore, the results showed that the maximum hardness and resistance to wear and corrosion of these NCs were improved. Tu et al. [33] examined the effect of channel shape and type of nanofluid on the maximum utilisation rate of waste heat. The obtained results revealed that the shape of the channel significantly increases the loss rate. Tu et al. [34] examined the effect of the shape, number and height of ribs and the volume fraction of nanoparticles on heat transfer in the heat exchanger channel. The results revealed that by increasing the volume fraction of TiO_2 nanoparticles, the performance of the heat exchanger improves. Wang et al. [35] examined the effect of pipe structure and hole shape on fluid flow inside two triangular and round tubes. The obtained results revealed that the structure of the triangular tube and the creation of a circular hole led to the improvement of the thermal efficiency of the nanofluid. Tang et al. [36] examined the effect of nanofluid concentration and magnetic field intensity on nanofluid heat transfer in a heat sink. The results revealed that the increase in the concentration of nanoparticles and the intensity of the magnetic field leads to the improvement of thermal properties in the studied structure.

Previous studies showed that various factors, such as volume fraction of nanoparticles, magnetic field, channel shape, size, etc., could affect the thermal and mechanical performance of the different composites. They showed that adding small amounts of NP reinforcements can lead to qualitative improvement in the strength and stiffness of various composites. Considering that the effect of reinforcing Al_2O_3 NP with different ratios of 2, 4, and 6% on the hardness of aluminum-based composites are not studied so far. And also, considering that the MD method can well estimate composites' thermal and mechanical behavior, in the present study, the thermal and mechanical properties of Al matrix composites reinforced with Al2O3 NP produced by powder metallurgy technology using the MD. In the first step, the pure aluminium composite was simulated. The reinforced aluminium composite with different volume fractions of Al_2O_3 NP was modeled in the next step. After ensuring the stability of the structures, increasing/decreasing the temperature in the simulated atomic structures was done, which caused the phase change and changes in the thermal behavior of atomic structures. The effect of the volume fraction of Al_2O_3 NP on the morphology, yield strength and RDF of Al matrix composites was studied. Finally, it is expected that the results obtained from MD simulations will be considered in the practical use of aluminium NCs reinforced with alumina nanoparticles in various industrial, engineering and medical uses to increase the performance and resistance of parts.

Table 1 – Parameters of Lennard-Jones potential function for particles in the present simulations [41].

Particle type	σ (Å)	ε (kcal/mol)
Aluminium	4.39	0.31
oxygen	3.166	0.1553

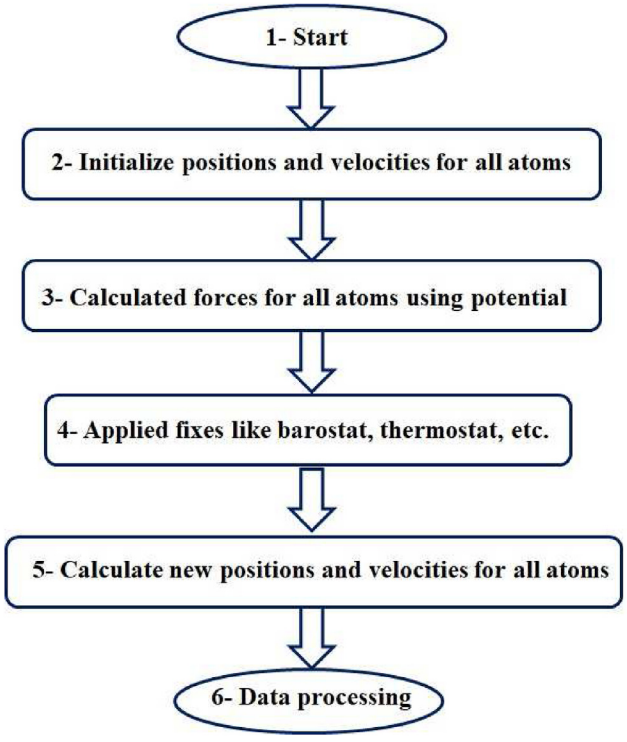

Fig. 1 – A general framework diagram of MD simulation [44].

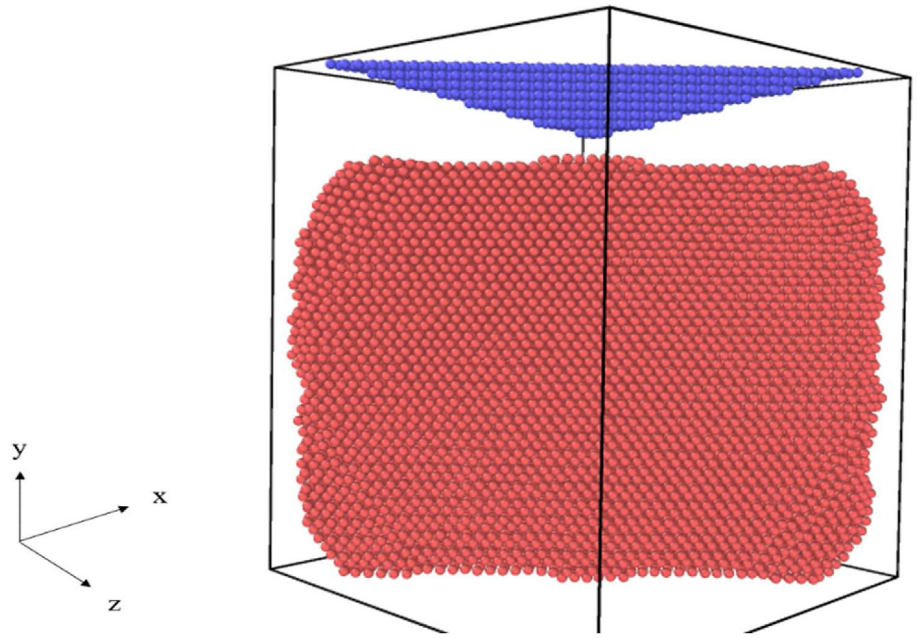

Fig. 2 – A view of the simulation box consists of a pure aluminium matrix and carbon indenter.

2. MD simulation

2.1. MD simulation details

In the MD simulations, Newton's second law is used to study the time evolution of systems. By solving Newton's equations of motion, the position of atom i (r_i) in a system of N atoms was obtained. By solving these equations for the particles that make up the movement system, all particles can be simulated with time. In this method, the force acting on a particle called i can be obtained via the potential function [37]. A better and faster method to calculate the equations of motion, which have high accuracy, is called the Verlet algorithm. In the MD simulation, the position and velocity values of the particles in the box are calculated using the velocity-Verlet equations and then creating a phase space for the studied system, including displacement and velocity quantities for each particle in the simulation [38,39].

The important factor that should be considered in the MD simulations is the potential function and interparticle forces definition. Force fields in MD simulations are one of the most important affecting parameters to obtain reliable results. More precisely, the force field was used in a conventional MD simulation to define the interatomic interactions. Using them, the potential energy of a system consisting of particles was calculated in the MD simulation. Lennard-Jones (LJ) and EAM potential function was used. LJ potential function was a simple mathematical model that approximated the interactions between a pair of neutral particles or molecules [40]. The most common relation of the LJ potential function was in the form of Eq. (1),

$$U_{LJ} = 4\varepsilon\left[\left(\frac{\sigma}{r}\right)^{12} - \left(\frac{\sigma}{r}\right)^{6}\right] \quad (1)$$

The aluminium composite was reinforced with Al_2O_3 NP. The interparticle interactions expressed in this research were Al–Al, Oxygen (O)–O, and Al–O. The amounts of aluminium and oxygen particles are according to Table 1 [36,37].

On the other hand, using the data in Table 1 and Eqs. (2) and (3), the values of σ and ε of each of the interactions among the present particles are calculated [41,42]:

$$\varepsilon_{ij} = \sqrt{\varepsilon_i \varepsilon_j} \quad (2)$$

$$\sigma_{ij} = \frac{\sigma_i + \sigma_j}{2} \quad (3)$$

The non-bonded potential function of EAM was used to express the interaction among metal particles used, such as aluminium and copper, and this quantity is presented by Eq. (4) [43]:

$$U_i = F_\alpha\left(\sum_{i\neq j}\rho_\beta(r_{ij})\right) + \frac{1}{2}\sum_{i\neq j}\phi_\beta(r_{ij}) \quad (4)$$

In this equation, F_α is a constant coefficient between 0 and 1. ρ_β is the factor caused by atomic charge density, and ϕ_β is the factor caused by the presence of particles in the simulation box. A general framework diagram of MD simulation is shown in Fig. 1.

2.2. Preparation of simulation system and definition of boundary conditions

The present research investigated the morphology, melting, and freezing behavior of aluminum matrix composites reinforced with Al_2O_3 NP produced by powder metallurgy technology using the MD simulation. Al matrix and Al_2O_3 NP are modeled with Avogadro software. In the first step, to create a pure Al structure, a simulation box with dimensions of

$100 \times 100 \times 100\ nm^3$ was filled with Al atoms. An example of a simulation box is shown in Fig. 2 to examine the mechanical properties, a carbon tip with a lattice constant of 2.5 Å is modeled with LAMMPS software. The angle of its vertices was 136° to each other for a certain time with a force of 6.24 eV. Periodic boundary conditions were applied to the sample in all directions. The atomic system was repeated in the selected directions by choosing periodic boundary conditions. Periodic boundary conditions were used to avoid problems of boundary effects caused by finite size in the simulated structure. Then, the structure was equilibrated at 300 K and 1 bar using the NPT ensemble. The Noose-Hoover thermostat will be used to control the temperature.

Then, increasing/decreasing the temperature in the simulated atomic structures was done, which caused the phase change and changes in the thermal behavior of atomic structures. Fig. 3 shows the graph of temperature changed over time. As seen in the graph, the temperature linearly increased with time until reaching the time of 0.82 ns. In the interval from 0.82 ns to 0.92 ns, the temperature was constant, and the hydrostatic pressure of 30 MPa was used to the sample and remains at a temperature of 830 K, which is called hot pressing. Then, the temperature linearly decreased with time and with a negative slope until reaching the initial temperature (300 K).

2.3. *The equilibration in simulated samples*

Fig. 4 shows the temperature changes in the simulated samples. As seen in this figure, the temperature in the simulated NC converged to 300 K after 1 ns. The observed convergence in temperature changes occurred in terms of reducing the atomic fluctuations in the NC, which reduced the mobility of particles, and thus the stability of overall atomic structure. On the other hand, the convergence in the temperature of the atomic structures showed the correctness of simulation settings applied to the atomic structures. To be more precise, the temperature convergence in atomic samples showed the correct process of atomic modeling and the appropriate choice of force field in the studied structure.

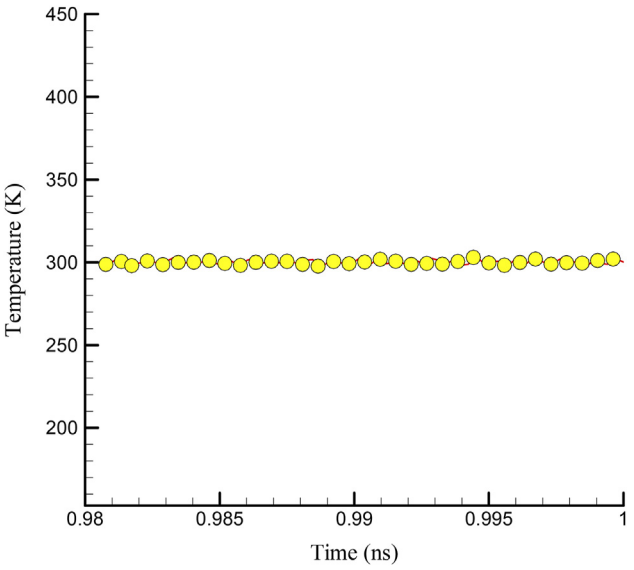

Fig. 4 – Temperature changes in the simulated atomic during 1 ns.

Examining potential energy changes in atomic samples is one of the other important things in MD simulations. Fig. 5 shows the potential energy changes in the simulated atomic sample during 1 ns. The numerical value of potential energy in an atomic sample showed its atomic stability. In such a way, in stable atomic structures and especially in solids, the numerical value of this quantity was negative. According to this graph, the structure of Al NC had good stability. From the numerical point of view, the value of potential energy in the simulated atomic sample was −130577 eV. The negative value in this quantity showed thermodynamic equilibrium and atomic stability in the studied NP.

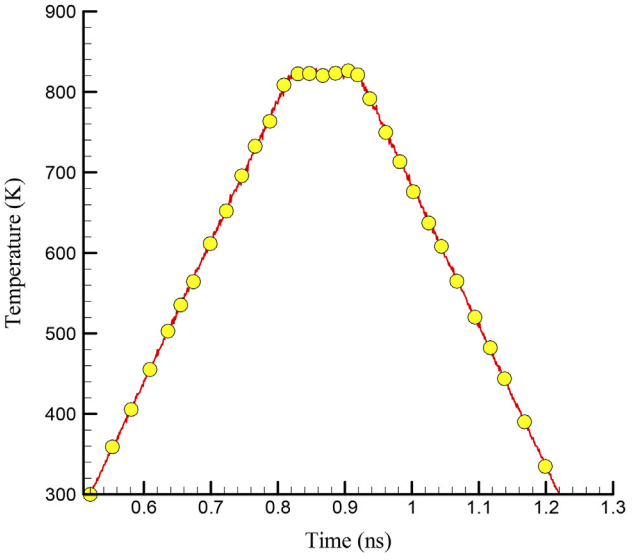

Fig. 3 – Temperature changes in the simulated atomic sample versus time.

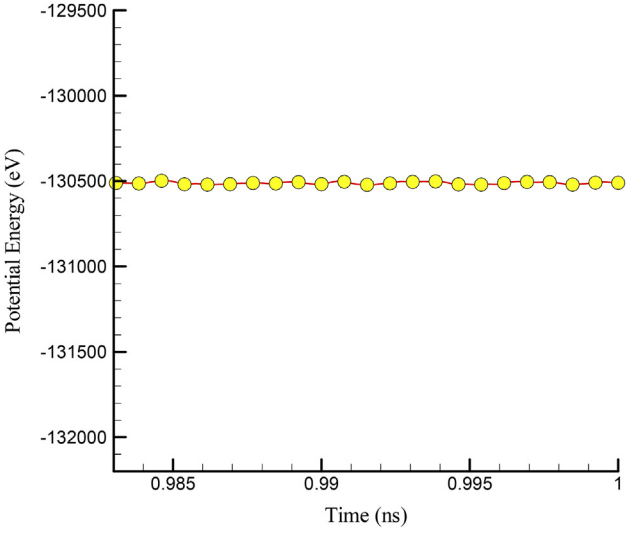

Fig. 5 – Changes in the potential energy of the simulated atomic sample versus time.

Table 2 – Specifications of prototype and reinforced with alumina.

Different samples	The length (nm)	The length (Å)	X1	X2	Y1	Y2	Xt	Yt
A0_M	11.1	106.564	86.7	12	11.9	87.9	−74.7	76
A2_M	8.8	87.565	81.6	18.7	20.78	81.7	−62.9	6.92
A4_M	8	80.186	79.2	22.7	23	79.9	−56.5	56.9
A6_M	7.8	77.996	77.9	22.3	22.3	77	−55.6	54.7

3. Results

After ensuring that the structure was equilibrated, the mechanical properties of simulated sample were reported. At this stage, a pyramidal carbon indenter pressed into the composite's surface and created a cavity. To calculate the hardness using the Vickers microhardness formula:

$$HV = \frac{1.854L}{d^2} \quad (7)$$

L is the force required in Newtons, and d is the gap diameter distance created by the indenter in millimetres. The coordinates of beginning and end point of the gap (Y_i and X_i) using the following equation:

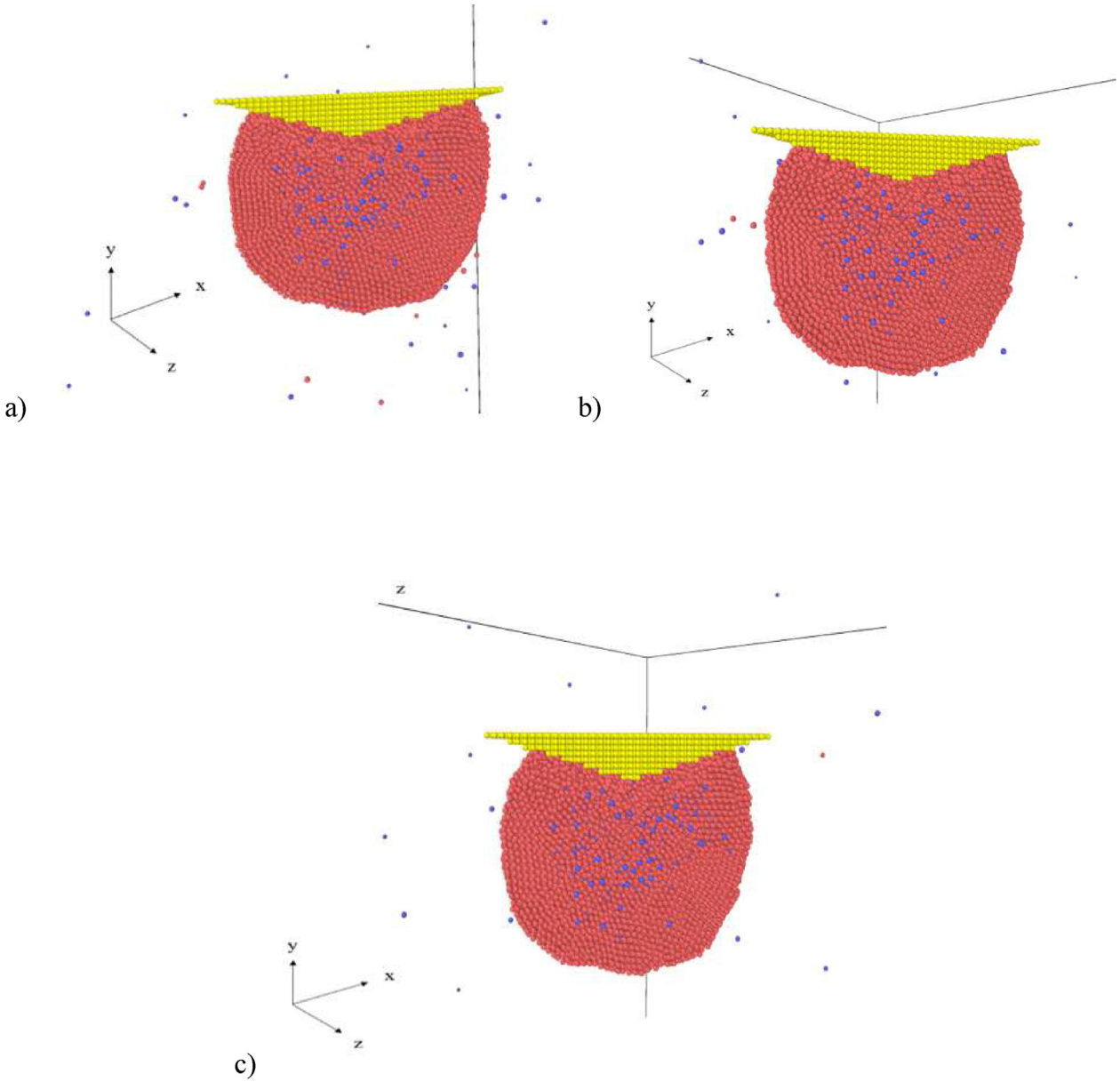

Fig. 6 – Microhardness test of aluminium composite reinforced with alumina with a) 2% b) 4% and c) 6% volume fraction.

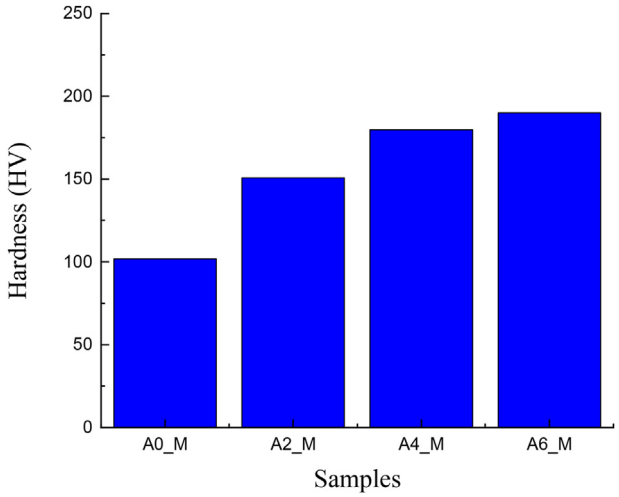

Fig. 7 – Changes in the hardness of the samples with different volume fractions of alumina NP.

$$D = \sqrt{(x_2 - x_1)^2 + (y_2 - y_1)^2} \quad (8)$$

The hardness of each sample is obtained in Vickers, and all steps are summarised in Table 2. Then, Al_2O_3 NP with volume fractions of 0, 2, 4 and 6% were added to the initial Al composite. The sample with 0, 2, 4 and 6% volume fractions are named A0_M, A2_M, A4_M and A6_M, respectively. Table 2 summarises how the Vickers microhardness test was calculated. This table reports the values (X_i, Y_i) of the initial and final coordinates of the largest gap created by the test indenter. Using equation (5), the desired gap size was obtained in angstroms, which can be seen in Table 2 to understand the gap size in nanometers better.

Then, the carbon indenter collides with the matrix, and its mechanical properties were checked. Microhardness test of aluminium composite reinforced with Al_2O_3 NP is shown in Fig. 6.

Fig. 7 shows the hardness of NC sample in terms of changes in the mass percentage ratio of alumina particles as reinforcement in the aluminium NC. Moreover, the hardness of pure NC is shown in the graph. It can be seen from the detailed analysis that in the pure NC, the hardness was equal to 101 Vickers, and by adding alumina NP with a mass ratio of 2%, the hardness value increased to 150 Vickers. Furthermore, in the mass ratio of 4% and 6% alumina NP, this value increased to 180 and 196 Vickers, respectively. Adding the alumina to the aluminium matrix increased the hardness of sample. To validate the results and accuracy of MD simulation in the current research, the simulation results were examined and compared with Ref. [45] results. Table 3 shows the numerical values resulting from this comparison in samples containing different mass ratios of nanoparticles. From the examination of the results, it can be stated that the accuracy was acceptable for the present research. The hardness of studied samples is obtained from Eq. (7).

Table 3 – Changes in the hardness of the samples with different volume fractions of alumina NP.

Different samples	Hardness (HV)
A0_M	101.7956
A2_M	150.763
A4_M	179.786
A6_M	190.023

According to the basic concepts of MD simulation, calculating the RDF was considered an efficient method of identifying different atomic structures. To be more precise, the maximum value of the RDF (peak) and the position of these maxima were different for multiple materials. Therefore, in the simulation of different atomic samples, the RDF of structure can be used to identify them. By examining the RDF, it will be possible to predict the thermodynamic properties of studied structure. In addition to the type of atomic structure, the phase of samples was effective in the RDF. Based on the shapes of radial distribution function, RDF in these samples had a peak at short distances and no peaks were observed at longer distances, and the value of g(r) converges to a constant value. The following formulation can express this function:

$$g(r) = \frac{\rho(r)\,dr}{\rho^{ideal}(r)\,dr} \quad (9)$$

Fig. 8 shows the RDF for pure aluminium at temperatures of 300 K. The initial peak created in this plot occurred near 3 Å. From the examination of this diagram, it can be concluded that the NC was in the solid phase at a temperature of 300 K, which indicated the appropriate balance of simulated atomic systems. The first peak for aluminium with 2% reinforcement occurred near 3 Å. From the examination of this graph, it can be concluded that the composition was in the solid phase at a temperature of 300 K, which indicates the proper balance of simulated atomic systems. In NCs reinforced with 4% nanoparticles, the maximum value of g(r) decreases compared to NCs reinforced with nanoparticles with 2%. The value of RDF for this type of NC was approximately 6.5 Å. Moreover, in NCs reinforced with 6% nanoparticles, compared to 2 and 4% reinforced NCs, it had decreased more. The value of RDF for this type of NC was approximately 6 Å. In general, it can be concluded that the RDF's maximum value decreases with the reinforcement increase.

Fig. 9 shows the mechanical test performed on the NC sample to obtain the yield stress. A tensile test was performed on the aluminium NC reinforced with alumina nanoparticles.

As shown in Fig. 10, the material's structure under the tensile test maintained its crystal structure even after 400-time steps, the plates were moving away from each other in a layered manner, and there was no sign of a necking point. That's why the yield stress of monocrystalline structures was much higher than materials in the amorphous or polycrystalline state in terms of the absence of voids or porosity in crystal structures. The stress-strain diagram for the pure NC is shown in Fig. 10. According to Fig. 10, the yield strength of pure aluminium NC with a single crystal structure at a strain of 0.5 was equal to 4.8 GPa. In the normal state, this yield stress value is a very large number because the materials in the natural state cannot be crystalline due to the presence of dislocations and disturbances in their structure. As can be

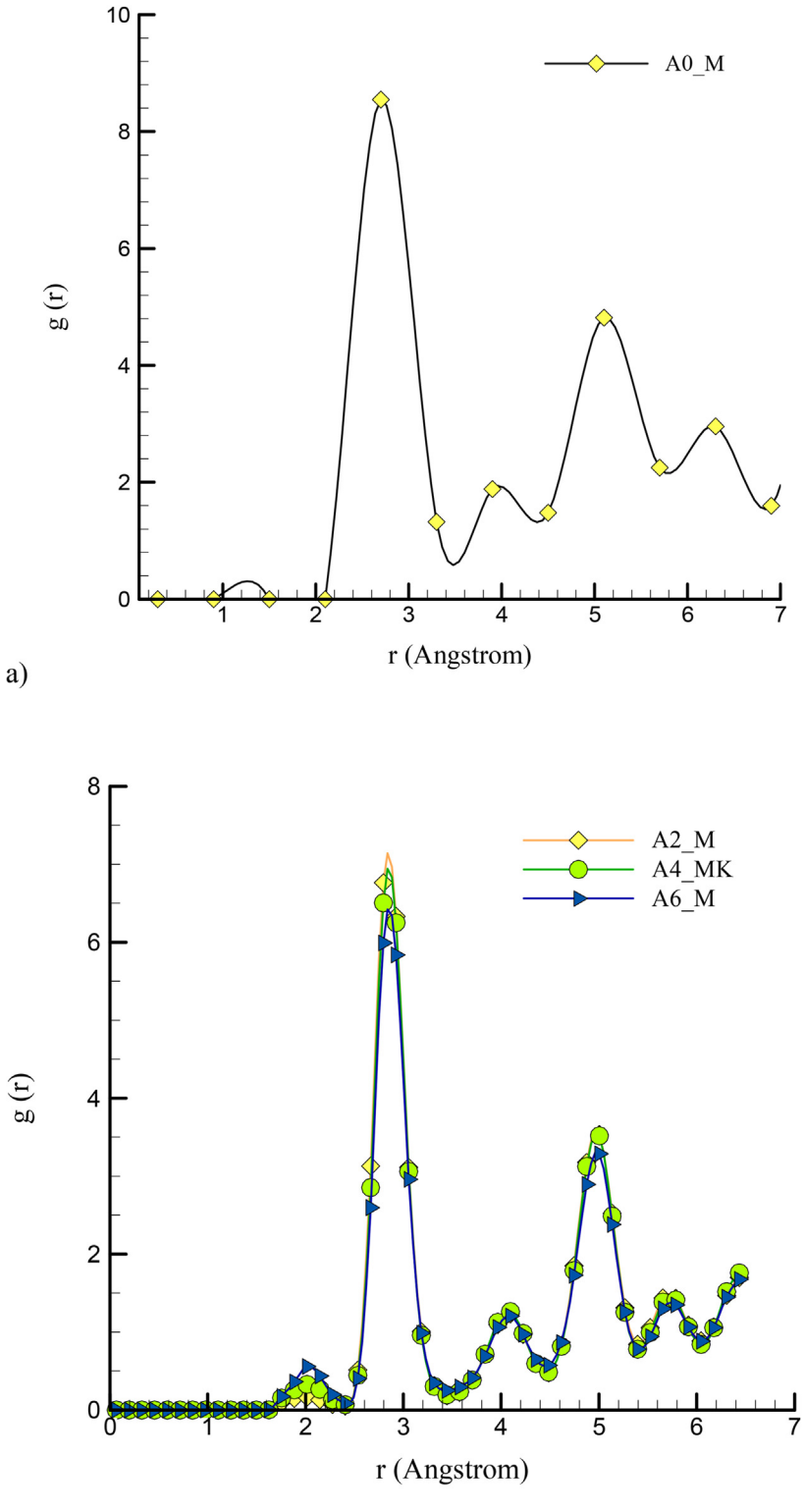

Fig. 8 – The RDF of a) pure and b) reinforced aluminium composite with different volume fractions.

seen, the maximum yield strength at a strain of 0.5 for the aluminium NC reinforced with 2% alumina NP was equal to 4 GPa. The yield strength in A2_M sample decreased compared to pure NC. By increasing volume fraction of nanoparticles to 4%, the yield stress equaled 3.7 GPa. By a further increase to 6%, the yield stress was reduced to 3.5 GPa. As the volume fraction of reinforcement increased in the crystal structure, the yield stress decreased.

Therefore, according to the present simulation results and the effect of nanoparticle volume fraction, it is possible to

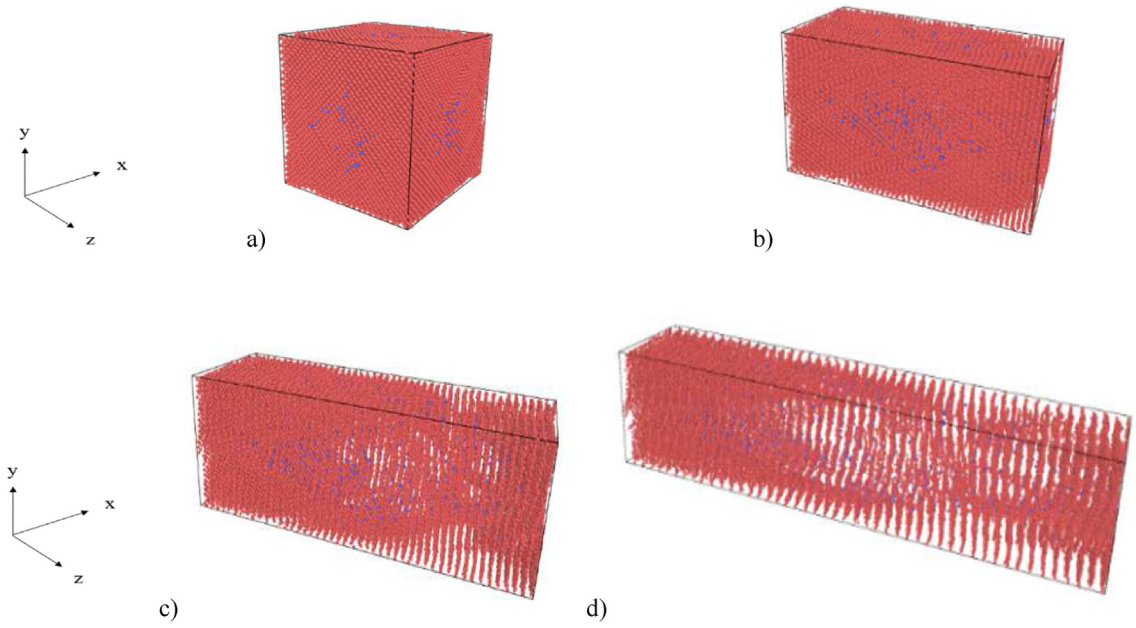

Fig. 9 – Tensile test on aluminium NC sample reinforced with alumina, a) at first, b) after 200, c) after 300, and d) after 400 time-steps.

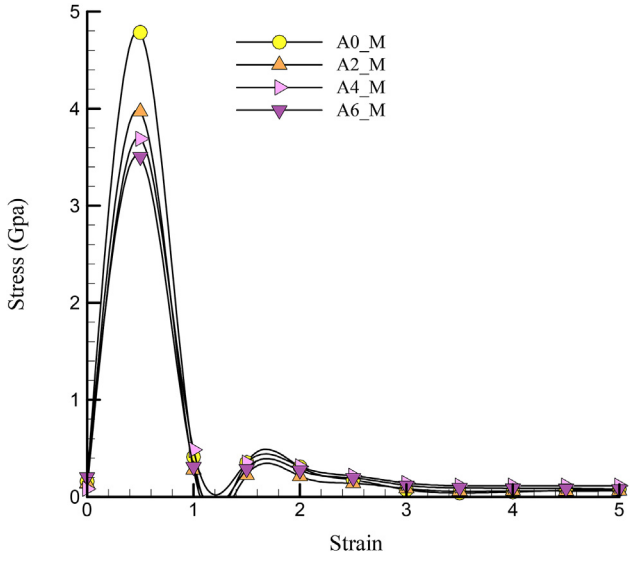

Fig. 10 – Stress-strain diagram reinforced NC with alumina nanoparticles.

strengthen the mechanical properties of metal-based nanocomposites.

4. Conclusion

This paper investigated the morphology and melting and freezing behavior of aluminium composites reinforced with Al_2O_3 NP produced by powder metallurgy technology with a hot press using the MD simulation and LAMMPS software. The results of MD simulations can be generally divided into two categories: the equilibration of atomic structures and mechanical tests. In the form of a list, the obtained results are vas follow.

- The temperature in the simulated NC converged to 300 K after a period of 1 ns.
- The numerical value of potential energy in an atomic sample showed its atomic stability. The potential energy in the simulated atomic sample converged to the numerical value of −130577 eV after 1 ns.
- In numerical studies, it was observed that in the pure NC, the hardness was equal to 100, and by adding alumina nanoparticles with a mass ratio of 4%, the hardness value increased to 1800. So, it can be concluded that adding alumina reinforcing nanoparticles to the aluminium matrix increased the hardness of sample.
- Calculating the RDF was a useful method to identify different atomic structures based on the basic concepts of MD simulation. By increasing the amount of reinforcement (in the present study, alumina nanoparticles), the maximum value (peak) of the radial distribution function decreases.
- As the volume fraction of reinforcement increased in the crystal structure, the yield stress decreased.

Finally, it is expected that the results obtained from MD simulations will be considered in the practical use of aluminium NCs reinforced with alumina nanoparticles in various industrial, engineering and medical uses.

Declaration of competing interest

The authors declare that they have no known competing financial interests or personal relationships that could have appeared to influence the work reported in this paper.

REFERENCES

[1] Zhang Z, Yang F, Zhang H, Zhang T, Wang H, Xu Y, …, Ma Q. Influence of CeO2 addition on forming quality and microstructure of TiCx-reinforced CrTi4-based laser cladding composite coating. Mater Char 2021;171. https://doi.org/10.1016/j.matchar.2020.110732.

[2] Zhang Z, Yang Q, Yu Z, Wang H, Zhang T. Influence of Y2O3 addition on the microstructure of TiC reinforced Ti-based composite coating prepared by laser cladding. Mater Char 2022;189. https://doi.org/10.1016/j.matchar.2022.111962.

[3] Rajeshkumar S, Subramanian AK, Prabhakar R. In vitro Anti-inflammatory activity of Silymarin/Hydroxyapatite/Chitosan Nanocomposites and its cytotoxic effect using Brine shrimp lethality assay: nanocomposite for biomedical applications. J Population Therapeutics Clin Pharmacol 2021;28(2). https://doi.org/10.47750/jptcp.2022.874.

[4] Müssig J, Graupner N. Test methods for fibre/matrix adhesion in cellulose fibre-reinforced thermoplastic composite materials: a critical review. Rev. Adhesion Adhesives 2021;8(No. 2):68–129.

[5] Lv B, Wang S, Xu T, Guo F. Effects of minor Nd and Er additions on the precipitation evolution and dynamic recrystallization behavior of Mg–6.0Zn–0.5Mn alloy. J Magnesium Alloys 2021;9(3):840–52. https://doi.org/10.1016/j.jma.2020.06.018.

[6] Andrzejczyk R, Gosz M. Magazyny ciepła ze złożem naturalnym i złożem na bazie materiałów zmiennofazowych. Materiały Budowlane 2016;(1):46–8.

[7] Dudina D, Georgarakis K, Aljerf M, Li Y, Braccini M, Yavari A, Inoue A. Cu-based metallic glass particle additions to significantly improve overall compressive properties of an Al alloy. Compos Appl Sci Manuf 2010;41(10):1551–7.

[8] Yu P, Zhang L, Zhang W, Das J, Kim K, Eckert J. Interfacial reaction during the fabrication of Ni60Nb40 metallic glass particles-reinforced Al based MMCs. Mater Sci Eng, A 2007;444(1–2):206–13.

[9] Yan S, Abhilash K, Tang L, Yang M, Ma Y, Xia Q, Guo Q, Xia H. Research advances of amorphous metal oxides in electrochemical energy storage and conversion. Small 2019;15(4):1804371.

[10] Demetriou MD, Wiest A, Hofmann DC, Johnson WL, Han B, Wolfson N, Wang G, Liaw PK. Amorphous metals for hard-tissue prosthesis. JOM (J Occup Med) 2010;62(2):83–91.

[11] Xie J, Chen Y, Yin L, Zhang T, Wang S, …, Wang L. Microstructure and mechanical properties of ultrasonic spot welding TiNi/Ti6Al4V dissimilar materials using pure Al coating. J Manuf Process 2021;64:473–80. https://doi.org/10.1016/j.jmapro.2021.02.009.

[12] Zhang P, Liu Z, Yue X, Wang P, Zhai Y. Water jet impact damage mechanism and dynamic penetration energy absorption of 2A12 aluminum alloy. Vacuum 2022;206:111532. https://doi.org/10.1016/j.vacuum.2022.111532.

[13] Zhang P, Liu J, Gao Y, Liu Z, Mai Q. Effect of heat treatment process on the micro machinability of 7075 aluminum alloy. Vacuum 2023;207:111574. https://doi.org/10.1016/j.vacuum.2022.111574.

[14] Zhang P, Liu Z, Liu J, Yu J, Mai Q, …, Yue X. Effect of aging plus cryogenic treatment on the machinability of 7075 aluminum alloy. Vacuum 2023;208:111692. https://doi.org/10.1016/j.vacuum.2022.111692.

[15] Deng H, Chen Y, Jia Y, Pang Y, Zhang T, Wang S, …, Yin L. Microstructure and mechanical properties of dissimilar NiTi/Ti6Al4V joints via back-heating assisted friction stir welding. J Manuf Process 2021;64:379–91. https://doi.org/10.1016/j.jmapro.2021.01.024.

[16] Yuhua C, Yuqing M, Weiwei L, Peng H. Investigation of welding crack in micro laser welded NiTiNb shape memory alloy and Ti6Al4V alloy dissimilar metals joints. Opt Laser Technol 2017;91:197–202. https://doi.org/10.1016/j.optlastec.2016.12.028.

[17] Trzepieciński T, Najm SM, Pepelnjak T, Bensaid K, Szpunar M. Incremental sheet forming of metal-based composites used in aviation and automotive applications. J Composites Sci 2022;6(10):295.

[18] Sun J, Simon S. The melting behavior of aluminum nanoparticles. Thermochim Acta 2007;463(1–2):32–40.

[19] Prabakaran R, Prasanna Naveen Kumar J, Mohan Lal D, Selvam C, Harish S. Constrained melting of graphene-based phase change nanocomposites inside a sphere. J Therm Anal Calorim 2020;139(2):941–52.

[20] Parameshwaran R, Deepak K, Saravanan R, Kalaiselvam S. Preparation, thermal and rheological properties of hybrid nanocomposite phase change material for thermal energy storage. Appl Energy 2014;115:320–30.

[21] Rong Y, He H, Zhang L, Li N, Zhu Y. Molecular dynamics studies on the strengthening mechanism of Al matrix composites reinforced by grapnene nanoplatelets. Comput Mater Sci 2018;153:48–56.

[22] Qiu Z, Zhang Z, Xiong Y, Luo X, Li Z, Zheng K, Hu W. Size effects of graphene sheets on the strengthening mechanism of Al-graphene composites: a molecular dynamics study. Applied Surface Science; 2022, 153546.

[23] Lee M, Kim J-H, Park J, Kim J, Kim W, Kim D. Fabrication of Ni–Nb–Ta metallic glass reinforced Al-based alloy matrix composites by infiltration casting process. Scripta Mater 2004;50(11):1367–71.

[24] D. Yadav, P. Gupta, and N. Yedla, "Nano-indentation of aluminium reinforced metallic glass composites: a molecular dynamics study." p. 012036.

[25] He H, Rong Y, Zhang L. Molecular dynamics studies on the sintering and mechanical behaviors of graphene nanoplatelet reinforced aluminum matrix composites. Model Simulat Mater Sci Eng 2019;27(6):065006.

[26] Mohammadi S, Montazeri A, Urbassek HM. Geometrical aspects of nanofillers influence the tribological performance of Al-based nanocomposites. Wear 2020;444:203117.

[27] Adnan A, Sun C, Mahfuz H. A molecular dynamics simulation study to investigate the effect of filler size on elastic properties of polymer nanocomposites. Compos Sci Technol 2007;67(3–4):348–56.

[28] Tabandeh-Khorshid M, Kumar A, Omrani E, Kim C, Rohatgi P. Synthesis, characterization, and properties of graphene reinforced metal-matrix nanocomposites. Compos B Eng 2020;183:107664.

[29] Yehia HM, Abu-Oqail A, Elmaghraby MA, Elkady OA. Microstructure, hardness, and tribology properties of the (Cu/MoS2)/graphene nanocomposite via the electroless deposition and powder metallurgy technique. J Compos Mater 2020;54(23):3435–46.

[30] Moustafa EB, Taha MA. Preparation of high strength graphene reinforced Cu-based nanocomposites via mechanical alloying method: microstructural, mechanical and electrical properties. Appl Phys A 2020;126(3):1–16.

[31] Arif S, Alam MT, Aziz T, Ansari AH. Morphological and wear behaviour of new Al-SiCmicro-SiCnano hybrid nanocomposites fabricated through powder metallurgy. Mater Res Express 2018;5(4):046534.

[32] Pal K, Navin K, Kurchania R. Study of structural and mechanical behaviour of Al-ZrO2 metal matrix nanocomposites prepared by powder metallurgy method. Mater Today Proc 2020;26:2714–9.

[33] Tu J, Qi C, Tang Z, Tian Z, Chen L. Experimental study on the influence of bionic channel structure and nanofluids on

power generation characteristics of waste heat utilisation equipment. Appl Therm Eng 2022;202:117893.
[34] Tu J, Qi C, Li K, Tang Z. Numerical analysis of flow and heat characteristic around micro-ribbed tube in heat exchanger system. Powder Technol 2022;395:562–83.
[35] Wang Y, Qi C, Ding Z, Tu J, Zhao R. Numerical simulation of flow and heat transfer characteristics of nanofluids in built-in porous twisted tape tube. Powder Technol 2021;392:570–86.
[36] Tang J, Qi C, Ding Z, Afrand M, Yan Y. Thermo-hydraulic performance of nanofluids in a bionic heat sink. Int Commun Heat Mass Tran 2021;127:105492.
[37] Rapaport DC, Rapaport DCR. The art of molecular dynamics simulation. Cambridge university press; 2004.
[38] Verlet L. Computer" experiments" on classical fluids. I. Thermodynamical properties of Lennard-Jones molecules. Phys Rev 1967;159(1):98.
[39] Swope WC, Andersen HC, Berens PH, Wilson KR. A computer simulation method for the calculation of equilibrium constants for the formation of physical clusters of molecules: application to small water clusters. J Chem Phys 1982;76(1):637–49.
[40] Lennard-Jones JE. Cohesion. Proc Phys Soc (1926-1948) 1931;43(5):461.
[41] Rappé AK, Casewit CJ, Colwell K, Goddard III WA, Skiff WM. UFF, a full periodic table force field for molecular mechanics and molecular dynamics simulations. J Am Chem Soc 1992;114(25):10024–35.
[42] Berendsen H, Grigera J, Straatsma T. The missing term in effective pair potentials. J Phys Chem 1987;91(24):6269–71.
[43] Daw MS, Baskes MI. Embedded-atom method: derivation and application to impurities, surfaces, and other defects in metals. Phys Rev B 1984;29(12):6443.
[44] M. Foroutan, and S. M. Fatemi, “Molecular dynamics simulations of systems containing nanostructures.”.
[45] Abedinzadeh R, Safavi S, Karimzadeh F. A comparative study on wear properties of nanostructured Al and Al/Al2O3 nanocomposite prepared by microwave-assisted hot press sintering and conventional hot pressing. J Mech Sci Technol 2015;29(9):3685–90.